Multiple alterations of platelet functions dominated by increased secretion in mice lacking Cdc42 in platelets

Irina Pleines,[1] Anita Eckly,[2] Margitta Elvers,[1] Ina Hagedorn,[1] Sandra Eliautou,[2] Markus Bender,[1] Xunwei Wu,[3] Francois Lanza,[2] Christian Gachet,[2] Cord Brakebusch,[3] and Bernhard Nieswandt[1]

[1]Department of Vascular Medicine, University Clinic, University of Würzburg and Rudolf Virchow Center, DFG Research Center for Experimental Biomedicine, Würzburg, Germany; [2]Inserm UMR-S949, Université de Strasbourg, Etablissement Français du Sang (EFS)–Alsace, Strasbourg, France; and [3]Biotec Research and Information Centre (BRIC), Biomedical Institute, University of Copenhagen, Copenhagen, Denmark

Platelet activation at sites of vascular injury is crucial for hemostasis, but it may also cause myocardial infarction or stroke. Cytoskeletal reorganization is essential for platelet activation and secretion. The small GTPase Cdc42 has been implicated as an important mediator of filopodia formation and exocytosis in various cell types, but its exact function in platelets is not established. Here, we show that the megakaryocyte/platelet-specific loss of Cdc42 leads to mild thrombocytopenia and a small increase in platelet size in mice. Unexpectedly, Cdc42-deficient platelets were able to form normally shaped filopodia and spread fully on fibrinogen upon activation, whereas filopodia formation upon selective induction of GPIb signaling was reduced compared with wild-type platelets. Furthermore, Cdc42-deficient platelets showed enhanced secretion of α granules, a higher adenosine diphosphate (ADP)/adenosine triphosphate (ATP) content, increased aggregation at low agonist concentrations, and enhanced aggregate formation on collagen under flow. In vivo, lack of Cdc42 resulted in faster occlusion of ferric chloride–injured arterioles. The life span of Cdc42-deficient platelets was markedly reduced, suggesting increased clearing of the cells under physiologic conditions. These data point to novel multiple functions of Cdc42 in the regulation of platelet activation, granule organization, degranulation, and a specific role in GPIb signaling. (*Blood*. 2010;115(16): 3364-3373)

Introduction

At sites of tissue trauma, platelets become activated and rapidly aggregate to form a plug that seals the wound and limits blood loss. On the other hand, platelet activation in pathologic situations can lead to thrombosis, causing myocardial infarction or stroke. Platelet activation by multiple signaling pathways leads to shape change, release of intracellularly stored granules, and spreading on immobilized ligands. Small GTPases of the Rho family, namely RhoA, Cdc42, and Rac1, are thought to play important roles in the cytoskeletal rearrangements occurring during platelet activation by facilitating the formation of stress fibers, filopodia and lamellipodia, respectively.[1] In platelets, signaling from G protein–coupled receptors, such as the thromboxane or thrombin receptors, as well as immunoreceptor tyrosine-based activation motif (ITAM)–coupled receptors (GPVI, CLEC-2) was shown to induce activation of Rho GTPases.[2,3]

Cdc42 is a small (~ 23 kDa) protein that cycles between a GDP-bound inactive and a GTP-bound active state.[4] Cdc42 is an important mediator of filopodia formation in various cell types. According to the "convergent elongation model," active Cdc42 induces activation of Wiskott-Aldrich Syndrome protein (WASP). WASP subsequently activates the ARP2/3 complex, thereby increasing actin turnover and initiating the formation of parallel actin bundles.[5-7] Furthermore, Cdc42 can also bind to and activate IRSp53, which recruits the Ena/vasodilator-stimulated phosphoprotein (VASP) family protein Mena, thus promoting filopodia elongation.[6,8] However, recent studies suggest that filopodia formation can also occur independently of Cdc42, involving most notably the novel Rho GTPase Rho-in filopodia (Rif) and the lipid-phosphatase–related protein-1 (LPR1).[9,10] Importantly, genetic targeting demonstrated that Cdc42 is not required for filopodia formation in embryonic fibroblastoid cells.[11]

Cdc42 has also been shown to be crucially involved in exocytosis in different cell types, such as neuroendocrine[12,13] and MIN6 beta cells,[14-16] as well as endothelial cells.[17,18] Furthermore, in the hematopoietic system, Cdc42 activation was postulated to be essential for antigen-stimulated degranulation in rat basophilic leukemia (RBL) mast cells.[19,20]

In platelets, 2 different types of releasable granules exist: α granules contain various proteins, including growth factors, and thrombogenic proteins, such as thrombospondin, fibronectin, and von Willebrand factor (VWF), which promote platelet activation and aggregation. Dense granules contain small molecules, notably adenosine diphosphate (ADP) and adenosine triphosphate (ATP), as well as histamine and serotonin.[21] Upon platelet activation with strong agonists, these granules are first centralized and then secreted,[22,23] which is essential for the recruitment of further platelets, thereby promoting platelet aggregation and thrombus growth.

Despite a number of previous studies on the function of Cdc42 in platelets, its role in platelet activation and cytoskeletal reorganization, as well as its impact on degranulation and thrombus formation, is currently unclear.

Submitted September 9, 2009; accepted January 11, 2010. Prepublished online as *Blood* First Edition paper, February 4, 2010; DOI 10.1182/blood-2009-09-242271.

The online version of this article contains a data supplement.

The publication costs of this article were defrayed in part by page charge payment. Therefore, and solely to indicate this fact, this article is hereby marked "advertisement" in accordance with 18 USC section 1734.

Methods

Generation of mice with *Cdc42*$^{-/-}$ platelets

To generate mice lacking Cdc42 specifically in megakaryocytes and platelets, mice containing the *Cdc42* gene flanked by loxP sites (*Cdc42*^{fl})[24] were crossed with mice carrying the platelet factor 4 (PF4)–cre transgene (PF4-cre^{+}).[25] In resulting Cdc42 (fl/fl)/PF4-cre^{+} mice, deletion of the *Cdc42* gene was confirmed by Western blot analysis of platelet lysates. Littermates (Cdc42(fl/fl)/PF4^{-}cre^{-}) served as controls. Mice were maintained on a mixed SV/129/C57/Bl-6 background. Animal studies were approved by the district government of Lower Franconia (Bezirksregierung Unterfranken).

Chemicals and reagents

The anesthetic drugs medetomidine (Pfizer), midazolam (Roche Pharma AG), and fentanyl (Janssen-Cilag GmbH) and the antagonists atipamezol (Pfizer), flumazenil, and naloxon (both from Delta Select GmbH) were used according to the regulation of the local authorities. ADP, phorbol 12-myristate 13-acetate (PMA), high-molecular-weight heparin, human fibrinogen (all from Sigma-Aldrich), α-thrombin (Boehringer Mannheim), anti-Cdc42 antibody (BD Biosciences), anti-cofilin antibody and anti-phosphocofilin antibody (from Cell Signaling), anti–human VWF and VWF–horseradish peroxidase (HRP) antibodies, anti–mouse IgG HRP (all from DAKO) and apyrase type III (Amersham/GE Healthcare) were purchased. Indomethacin was purchased from a local pharmacy. Botrocetin was purified as described.[26] Mouse recombinant VWF was provided by Cécile Denis and Peter Lenting (Inserm U770, Université Paris-Sud, Paris, France). Collagen-related peptide (CRP) was generated as described.[27] The antibody against the activated form of integrin $\alpha_{IIb}\beta_3$ (JON/A-PE) was from Emfret Analytics. All other antibodies were generated and modified in our laboratory as previously described.[28]

Platelet preparation

Mice were bled under isufluran anesthesia from the retro-orbital plexus. A total of 500 μL of blood per mouse was collected in a tube containing 7.5 U/mL heparin and platelet-rich plasma (PRP) was obtained by centrifugation at 300*g* for 10 minutes at room temperature (RT). For preparation of washed platelets, PRP was washed at 1000*g* for 8 minutes at RT, and the pellet was resuspended in modified Tyrode-HEPES buffer (134mM NaCl, 0.34mM Na_2HPO_4, 2.9mM KCL, 12mM $NaHCO_3$, 5mM HEPES, 2mM $CaCl_2$, 1mM $MgCl_2$, 5mM glucose, and 0.35% bovine serum albumin [BSA; pH 7.4]) in the presence of prostacyclin (0.1 μg/mL) and apyrase (0.02 U/mL). Platelets were finally resuspended in the same buffer without prostacyclin (pH 7.4; 0.02 U/mL apyrase) and incubated at 37°C for 30 minutes before use.

Platelet spreading on fibrinogen and CRP

Cover slips were coated with 100 μg of human fibrinogen or CRP and blocked with phosphate-buffered saline (PBS) 1% BSA. After rinsing with Tyrode-HEPES buffer, washed platelets (100 μL with 0.03×10^6 platelets/μL) were added and incubated at RT for the indicated time periods. The cover slips were rinsed again, and platelets were visualized with a Zeiss Axiovert 200 inverted microscope (100×/1.4 oil objective). Digital images were recorded using a CoolSNAP-EZ camera (Visitron) and analyzed off-line using Metavue software.

Platelet spreading on VWF

Cover slips were coated with anti–human VWF antibody (DAKO), followed by incubation with 10 μg/mL mouse recombinant VWF and blocking with PBS 1% BSA. Washed platelets were incubated with integrilin (40 μg/mL) and botrocetin (2 μg/mL) and allowed to adhere for 20 minutes. Samples were rinsed with PBS, fixed with 2.5% glutaraldehyde, and processed for scanning electron microscopy (SEM).

Transmission electron microscopy

Resting or activated platelets were fixed with 2.5% glutaraldehyde in 0.1M cacodylate buffer (pH 7.2) containing 2% sucrose and embedded in epon. Thin sections were stained with uranyl acetate and lead citrate and examined at 120 kV under a CM120 BioTWIN transmission electron microscope (FEI). Pictures were taken with a Megaview camera (Olympus SIS).

SEM

Platelets in suspension were fixed with 2.5% glutaraldehyde and allowed to adhere to poly-L-lysine–coated coverslips. Spread platelets were fixed with 2.5% glutaraldehyde. Samples were dehydrated, air-dried, sputtered with gold, and examined at 5 kV under a SIRION scanning electron microscope (FEI). Pictures were analyzed using XL control soft imaging system software. To visualize intracellular cytoskeletal filaments, spread platelets were incubated with 0.75% Triton X-100 in PHEM containing 0.1% glutaraldehyde, 5μM phalloidin, and 30μM taxol. Cytoskeletons were fixed in 2% paraformaldehyde. Samples were treated with 0.2% tannic acid for 20 minutes, followed by 0.5% osmium for 5 minutes and prepared for SEM as described.

Aggregometry

Light transmission was measured on a Fibrintimer 4 channel aggregometer (APACT Laborgeräte und Analysensysteme) using PRP or washed platelets (200 μL with 0.3×10^6 platelets/μL). Platelet aggregation using PRP was induced by addition of CRP, collagen, U46619, or ADP. Thrombin-induced aggregation was performed with washed platelets. Platelet agglutination was induced in washed platelets by addition of 5 μg/mL botrocetin and 10 μg/mL human VWF in the presence of 40 μg/mL integrilin.

Flow cytometry and Western blot analysis

A total of 50 μL of blood was washed twice in PBS and diluted 1:20 in Tyrode-HEPES buffer containing 2mM $CaCl_2$. Samples were activated with agonists at the indicated concentrations, stained with fluorophore-conjugated monoclonal antibodies at saturating concentrations for 10 minutes at 37°C and analyzed on a FACSCalibur (BD Biosciences). For Western blot analysis, blotted platelet lysates were probed with anti-Cdc42 antibody (1 μg/mL) and anti–mouse IgG-HRP. Proteins were visualized by enhanced chemiluminescence (ECL). GPIIIa levels were used as loading control.

Adhesion under flow conditions

Cover slips were coated with 0.25 mg/mL fibrillar type I collagen (Nycomed) and blocked with 1% BSA. Perfusion of heparinized whole blood was performed as described.[29] Before perfusion, anticoagulated blood was incubated with Dylight-488–conjugated anti-GPIX derivative (0.2 μg/mL) at 37°C for 5 minutes. Aggregate formation was visualized with a Zeiss Axiovert 200 inverted microscope (40×/0.60 objective) equipped with a CoolSNAP-EZ camera (Visitron). Phase-contrast and fluorescence pictures were recorded with a CoolSNAP-EZ camera (Visitron), and analyzed off-line using Metavue software.

Measurement of PF4, ATP, and serotonin release

Washed platelets at a concentration of 0.4×10^6/μL were activated with the indicated agonists for 2 minutes at 37°C and immediately centrifuged. PF4 and serotonin were quantified using a mouse PF4 enzyme-linked immunosorbent assay (ELISA; RayBiotech) and a mouse serotonin ELISA (IBL) according to the manufacturers' protocol. ATP in 10 μL of supernatant was quantified as described.[3]

Measurement of platelet PF4, P-selectin, VWF, and serotonin content

Washed platelets were lysed and contents of PF4, P-selectin, and serotonin were determined by ELISA (see "Measurement of PF4, ATP, and serotonin

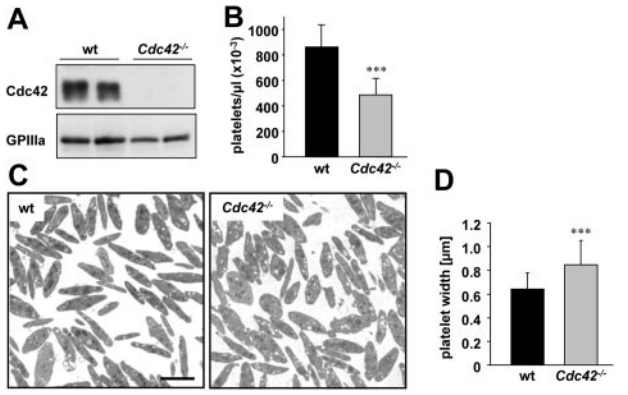

Figure 1. *Cdc42*$^{-/-}$ mice display mild thrombocytopenia. (A) Western blot analysis of Cdc42 expression in wild-type and *Cdc42*$^{-/-}$ platelets. GPIIIa expression was used as loading control. (B) Peripheral platelet counts (n = 6 per group). Error bars: wt, 860.95 ± 176.94; Cdc42$^{-/-}$, 489.41 ± 128.91 ($\times 10^3$)/µL; ***$P < .001$. (C) Representative TEM pictures from wild-type and *Cdc42*$^{-/-}$ platelets. Scale bar equals 2 µm. (D) *Cdc42*$^{-/-}$ platelets are increased in size. Mean platelet width of wild-type and *Cdc42*$^{-/-}$ platelets (n = 25 per group). Error bars: wt, 0.64 ± 0.14; Cdc42$^{-/-}$, 0.85 ± 0.21 [µm]; ***$P < .001$.

release"). VWF content was measured by ELISA using uncoupled and peroxidase-coupled hVWF antibodies (DAKO).

Measurement of total platelet nucleotide content

Platelets were suspended in Tyrode albumin buffer, and proteins were precipitated with ice-cold 6.6 N perchloric acid. After centrifugation, nucleotides were isolated from supernatants with trioctylamine and freon (vol/vol) and measured by high-performance liquid chromatography (HPLC) as described.[30]

Determination of platelet life span

Mice were injected intravenously with Dylight-488–conjugated anti-GPIX Ig derivative (0.5 µg/g body weight). At 1 hour after injection (day 0), as well as at the other indicated time points, 50 µL of blood were collected and the percentage of GPIX$^+$ platelets was determined by flow cytometry.

Bleeding time

Tail bleeding time experiments were performed as described.[31]

Intravital microscopy of thrombus formation in $FeCl_3$-injured mesenteric arterioles

Intravital microscopy was performed as described.[31] Briefly, mice were anesthetized, and the mesentery was exteriorized. Injury was induced by topical application of 20% $FeCl_3$. Arterioles were visualized at 10× with a Zeiss Axiovert 200 inverted microscope (10×/0.25 objective) equipped with a 100-W HBO fluorescent lamp source and a CoolSNAP-EZ camera (Visitron). Digital images were recorded and analyzed off-line using Metavue software. Adhesion and aggregation of fluorescently labeled platelets in arterioles was monitored for 40 minutes or until complete occlusion occurred (blood flow stopped for more than 1 minute).

Data analysis

Results are shown as mean plus or minus SD from at least 3 individual experiments per group. Statistical analysis between wild-type and *Cdc42*$^{-/-}$ groups were assessed by the Mann-Whitney *U* test. *P* values less than .05 were considered statistically significant.

Results

Constitutive deletion of the *Cdc42* gene results in embryonic lethality in mice.[32] To study the function of Cdc42 in platelets, mice carrying a *Cdc42* gene flanked by loxP sites[24] were crossed with transgenic mice expressing Cre recombinase under the control of the megakaryocyte- and platelet-specific platelet factor (PF) 4 promoter.[25] In resulting Cdc42 (fl/fl cre$^+$) mice, gene deletion was induced intrinsically upon induction of the PF4 promoter during megakaryocyte maturation. Cdc42 (fl/fl cre$^-$, further referred to as wild-type) mice derived from the same litters served as controls. The absence of Cdc42 protein in Cdc42 (fl/fl cre$^+$, further referred to as *Cdc42*$^{-/-}$) mice was confirmed by Western blot analysis of platelet lysates using GPIIIa expression levels as loading control (Figure 1A). Megakaryocyte- and platelet-specific deletion of Cdc42 resulted in a moderate thrombocytopenia with platelet counts ranging between 50% and 80% of controls (Figure 1B), indicating a significant but not essential role for Cdc42 in megakaryocyte differentiation and/or platelet formation. Platelet size was moderately increased in *Cdc42*$^{-/-}$ animals, as revealed by transmission electron microscopy (TEM) and determination of the platelet width (Figure 1C-D), as well as by flow cytometric assessment of the forward scatter signal (Table 1). Expression of major platelet surface receptors was similar to controls with exception of subunits of the GPIb/V/IX complex, where expression levels were decreased by approximately 20% compared with wild-type platelets (Table 1).

Cdc42$^{-/-}$ platelets form filopodia and fully spread on fibrinogen

Cdc42 has been demonstrated to be crucial for filopodia formation in various cell types, and also an essential role for filopodia formation in platelets has been reported.[33] To test this directly, wild-type and *Cdc42*$^{-/-}$ platelets were allowed to spread on a fibrinogen-coated surface in the presence of thrombin (0.01 U/mL final concentration: Figure 2A-B). Surprisingly, *Cdc42*$^{-/-}$ platelets formed filopodia to a similar extent and with similar kinetics as wild-type platelets, and after 30 minutes, the rate of fully spread platelets was comparable between the 2 groups (Figure 2B; supplemental Videos 1 and 2, available on the *Blood* Web site; see the Supplemental Materials link at the top of the online article). The filopodia formed in *Cdc42*$^{-/-}$ platelets (Figure 2A bottom panel) were microscopically indistinguishable from those formed in wild-type platelets (Figure 2A top panel). Likewise, *Cdc42*$^{-/-}$ and wild-type platelets exhibited similar morphology and filopodia structure upon adhesion on fibrinogen under either unstimulating conditions (Figure 2C) or upon activation with 5µM ADP (data not

Table 1. Platelet glycoprotein expression in wild-type and *Cdc42*$^{-/-}$ mice

	Wild-type, MFI	*Cdc42*$^{-/-}$, MFI
Mean FSC	345 ± 21	440 ± 37
GPIb	389 ± 8	306 ± 11
GPV	260 ± 4	212 ± 3
GPIX	403 ± 13	343 ± 2
CD9	1443 ± 21	1226 ± 10
GPVI	61 ± 2	52 ± 3
α2	90 ± 4	90 ± 8
β1	162 ± 10	183 ± 9
$\alpha_{IIb}\beta_3$	560 ± 63	513 ± 38

Expression of glycoproteins on the platelet surface was determined by flow cytometry. Diluted whole blood from the indicated mice was incubated with fluorescein isothiocyanate–labeled antibodies at saturating concentrations for 15 minutes at room temperature, and platelets were analyzed directly. Results are expressed as mean fluorescence intensity ± SD for 6 mice per group. Mean platelet size (mean FSC) was determined by FSC characteristics.

MFI indicates mean fluorescence intensity; FSC, forward scatter; and GP, glycoprotein.

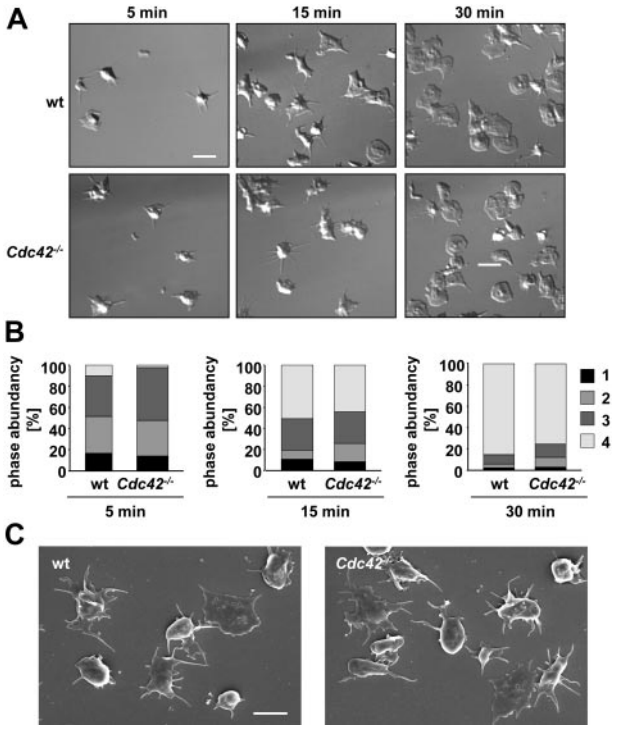

Figure 2. *Cdc42*$^{-/-}$ platelets are able to form filopodia and to spread on fibrinogen. (A) Washed platelets from the indicated mice were allowed to adhere and spread on immobilized human fibrinogen (100 μg/mL) upon activation with thrombin (0.01 U/mL). Differential interference contrast (DIC) images were taken at the indicated time points (5, 15, and 30 minutes), representative of 4 individual experiments. Scale bar equals 5 μm. (B) Statistical analysis of the percentage of spread *Cdc42*$^{-/-}$ and wild-type platelets observed at different spreading stages at the indicated time points. 1 indicates roundish, no filopodia, no lamellipodia; 2, only filopodia; 3, filopodia and lamellipodia; and 4, full spreading, only lamellipodia. Scale bar equals 5 μm. (C) Scanning electron microscopy (SEM) of wild-type and *Cdc42*$^{-/-}$ platelets upon spreading on 100 μg/mL fibrinogen without agonist stimulation. Scale bar equals 2.5 μm.

shown). These data demonstrate that Cdc42 is not required for filopodia formation and spreading of platelets on a fibrinogen matrix.

For a more detailed analysis of the cytoskeletal ultrastructure in Cdc42-deficient platelets, scanning electron microscopic studies were performed (Figure 3). Apart from their increased size, no morphologic differences between resting *Cdc42*$^{-/-}$ and wild-type platelets were noted (Figure 3A); moreover, thrombin-induced filopodia (30 minutes) were not different in length or shape between the 2 groups (Figure 3B). To also study the impact of Cdc42 deficiency on platelet shape change in suspension, washed platelets were activated with ADP or thrombin under stirring conditions for 15 seconds and visualized by SEM (Figure 3C). Under these conditions, *Cdc42*$^{-/-}$ and control platelets displayed similar morphology, including a contracted cell body and the formation of numerous filopodia.

Taken together, these results reveal normal formation and structure of filopodia and normal spreading morphology as well as normal agonist-induced shape change in *Cdc42*$^{-/-}$ platelets.

Cdc42$^{-/-}$ platelets exhibit reduced filopodia extension after adhesion on immobilized VWF

We next evaluated the platelet response upon adhesion to a mouse VWF–coated surface under conditions of integrin $\alpha_{IIb}\beta_3$ blockade (Figure 3D). Under these conditions, a GPIb-specific signal is triggered, resulting in shape change that is limited to contraction of the cell body and filopodia formation.[34] In contrast to control platelets, which efficiently extended filopodia (75% showing more than 3 filopodia), *Cdc42*$^{-/-}$ platelets exhibited a profound decrease in the ability to form filopodia, with most displaying no (25%) or less than 4 (50%) filopodia per platelet and the inability to contract their cell body. Importantly, the observed defect in filopodia formation in *Cdc42*$^{-/-}$ platelets was not caused by decreased GPIb

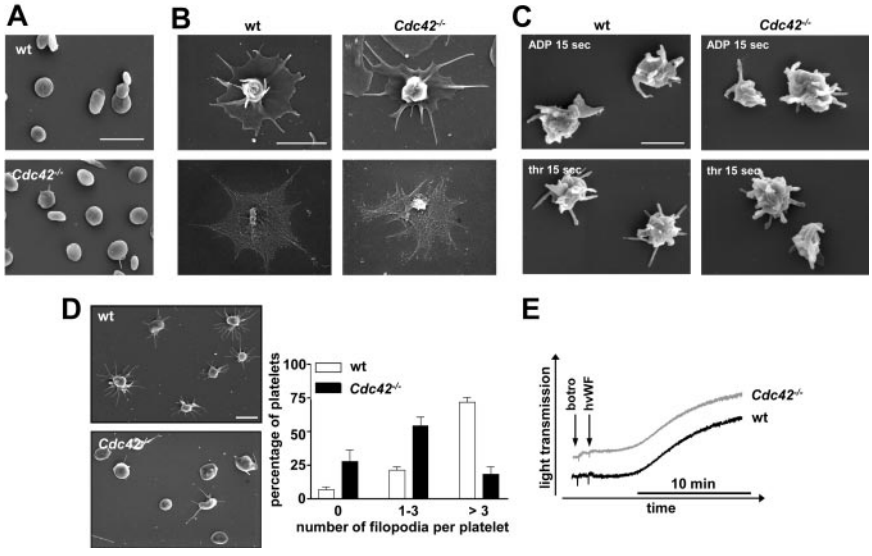

Figure 3. SEM analysis of *Cdc42*$^{-/-}$ platelets. (A-C) Normal ultrastructure of *Cdc42*$^{-/-}$ platelets. (A) Resting platelets immobilized on poly-L-lysine. Scale bar equals 5 μm. (B) Spread *Cdc42*$^{-/-}$ and wild-type platelets upon activation with 0.01 U/mL thrombin on human fibrinogen (100 μg/mL). Top panels show SEM of intact platelets. Bottom panels show visualization of the actin cytoskeleton upon denudation of the plasma membrane. Scale bar equals 2 μm. (C) Morphology of *Cdc42*$^{-/-}$ and wild-type platelets in suspension at 15 seconds after activation with thrombin (0.1 U/mL; top panels) or ADP (5μM; bottom panels). Scale bar equals 1 μm. (D) *Cdc42*$^{-/-}$ platelets exhibit reduced filopodia extension upon adhesion on mouse VWF (20 minutes). Left panels show representative images of 5 experiments. Scale bar equals 2.5 μm. Right panel shows statistical evaluation of filopodia formation according to the number of extensions per platelet (0, 1-3, > 3) in 5 different fields corresponding to a total surface of 9215 μm^2. The results are mean values ± SD (n = 5 per group). (E) Unaltered agglutination of *Cdc42*$^{-/-}$ platelets. Washed *Cdc42*$^{-/-}$ and wild-type platelets were stimulated with botrocetin (5 μg/mL) and human VWF (10 μg/mL) in presence of 40 μg/mL integrilin under stirring conditions and agglutination was monitored over 15 minutes on a Fibrintimer 4 channel aggregometer (APACT Laborgeräte und Analysensysteme). Curves are representative of 3 individual experiments.

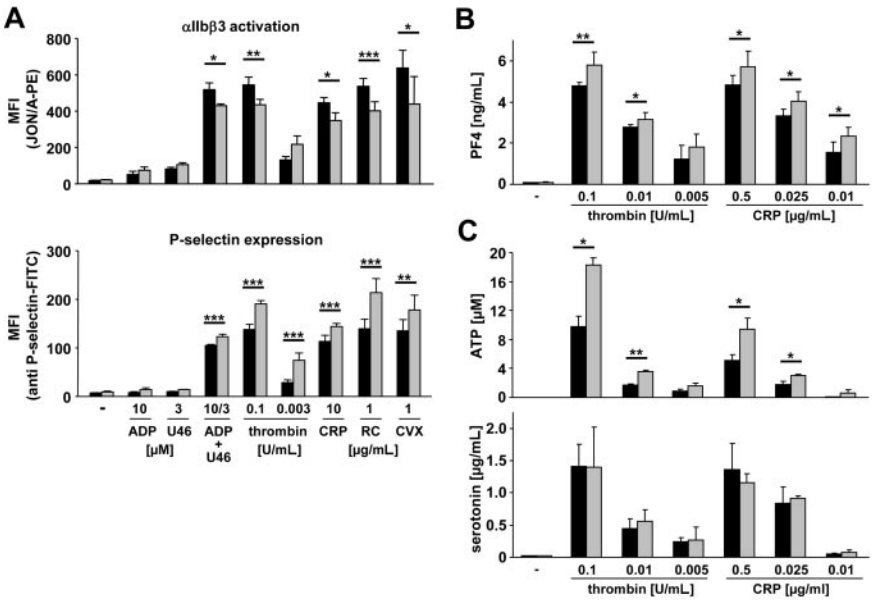

Figure 4. Increased secretion in *Cdc42*$^{-/-}$ platelets upon activation. (A) Flow cytometric analysis of $\alpha_{IIb}\beta_3$ integrin activation (binding of JON/A-PE; top panel) and degranulation-dependent P-selectin exposure (bottom panel) in response to the indicated agonists from wild-type (■) or *Cdc42*$^{-/-}$ (▨) platelets. U46 indicates U46619. Results are mean fluorescent intensities (MFIs) ± SD of 6 mice per group. *P* values from left to right: top, *.015; **.008; *.012; ***< .001; *.017; bottom, ***< .001; **.008. (B) Measurement of released PF4 in the supernatant of resting or activated wild-type (■) and *Cdc42*$^{-/-}$ (▨) platelets. Results are given as mean PF4 concentration (ng/mL) ± SD (n = 4 per group). *P* values from left to right: **.003; *.026; *.014; *.011; *.010. (C) Measurement of released ATP (top panel) and serotonin (bottom panel) in the supernatant of resting or activated wild-type (■) and *Cdc42*$^{-/-}$ (▨) platelets. Results are given as mean ATP concentration (μM) and mean serotonin concentration (μg/mL) ± SD (n = 4 per group). (Top) *P* values from left to right: *.012; **.002; *.019; *.015.

expression levels of the protein because GPIb-dependent agglutination by botrocetin and human VWF was unaltered in the mutant platelets compared with that of controls (Figure 3E). Furthermore, filopodia formation upon static adhesion on CRP, which acts via GPVI and has been proposed to induce similar signaling events compared with GPIb, occurred to a similar extent in wild-type and *Cdc42*$^{-/-}$ platelets (supplemental Figure 1). Together, these results suggest a specific role of Cdc42 in filopodia formation downstream of GPIb in a signaling pathway differing from that triggered by GPVI or G protein–coupled receptors.

Increased secretion in *Cdc42*$^{-/-}$ platelets

Cdc42 is required for exocytotic processes in various cell types, such as mast cells, where it was shown to be crucially involved in antigen-stimulated secretion.[19,20] To address a possible role of Cdc42 in this process in platelets, we tested the ability of *Cdc42*$^{-/-}$ and wild-type platelets to release granules upon agonist activation (Figure 4). In parallel, activation of the main platelet integrin, $\alpha_{IIb}\beta_3$, was assessed.[35] Surprisingly, and in contrast to studies in other cell types, we found that P-selectin expression was not decreased but markedly increased in *Cdc42*$^{-/-}$ compared with wild-type platelets in response to all tested strong agonists (Figure 4A; bottom panel). In line with this, release of PF4, a protein specifically stored in platelet α granules, was also moderately but significantly increased in *Cdc42*$^{-/-}$ platelets upon activation compared with the control (Figure 4B). In contrast, integrin $\alpha_{IIb}\beta_3$ activation in response to strong stimuli was moderately decreased in *Cdc42*$^{-/-}$ platelets compared with wild-type (Figure 4A top panel). The increased levels of P-selectin expression and PF4 release in *Cdc42*$^{-/-}$ platelets indicated enhanced secretion of α granules. To test whether release of dense granules was also affected, we measured the amount of released ATP and serotonin upon agonist stimulation (Figure 4C). We found strongly increased ATP release in *Cdc42*$^{-/-}$ compared with wild-type platelets in response to thrombin and CRP (Figure 4C top panel), whereas serotonin release was not significantly different compared with wild-type (Figure 4C bottom panel).

TEM revealed comparable numbers of α and dense granules in *Cdc42*$^{-/-}$ and control platelets (data not shown) and no significant differences between wild-type and mutant cells were found in the total amount of the representative α-granular proteins P-selectin, PF4, and VWF (supplemental Figure 2A-C). Thus, together with the results from flow cytometry and PF4 release, these data support the hypothesis of increased α granule–dependent secretion in *Cdc42*$^{-/-}$ platelets.

In contrast, the amount of dense granule-specific ADP and ATP was significantly increased in resting *Cdc42*$^{-/-}$ platelets (wild-type: ADP = 1.28 ± 0.02; ATP = 4.61 ± 0.14 vs *Cdc42*$^{-/-}$: ADP = 2.0 ± 0.112, ATP = 5.56 ± 0.12; $P = .025$ and $P < .001$; supplemental Figure 2D), whereas levels of serotonin were not significantly altered (supplemental Figure 2E). The observed increased ADP/ATP content may to a certain extent be related to the increased size of *Cdc42*$^{-/-}$ platelets compared with the control. Alternatively, specific alterations in the process of granule packing may also contribute to the observed enhanced ADP/ATP secretion from dense granules in *Cdc42*$^{-/-}$ platelets.

Enhanced aggregation of *Cdc42*$^{-/-}$ platelets at low agonist concentrations

To study the functional consequences of the increased granule content and secretion and slightly decreased $\alpha_{IIb}\beta_3$ integrin activation in *Cdc42*$^{-/-}$ platelets, we performed aggregation studies (Figure 5). Whereas the overall maximal aggregatory response to all tested agonists was similar in *Cdc42*$^{-/-}$ and wild-type platelets, strongly enhanced aggregation of *Cdc42*$^{-/-}$ platelets was seen at threshold concentrations of the thromboxane A2 analog U46619, CRP, and collagen (Figure 5B-C). The degree of aggregation in response to these agonists is known to be strongly dependent on released secondary mediators, indicating that the enhanced secretion of *Cdc42*$^{-/-}$ platelets accounted for this effect. Consistent with this, aggregation in response to the weak agonist ADP, which alone does not induce degranulation, was similar in *Cdc42*$^{-/-}$ and wild-type platelets (Figure 5A,C). No significant difference in aggregation between wild-type and mutant platelets could be detected in response to thrombin (Figure 5A,C). Notably, *Cdc42*$^{-/-}$ platelets did not aggregate spontaneously upon addition of epinephrine (data not shown), indicating that they were not per se in a preactivated state under the in vitro conditions used here.

Taken together, these data revealed increased agonist-induced secretion and subsequent aggregation in *Cdc42*$^{-/-}$ platelets.

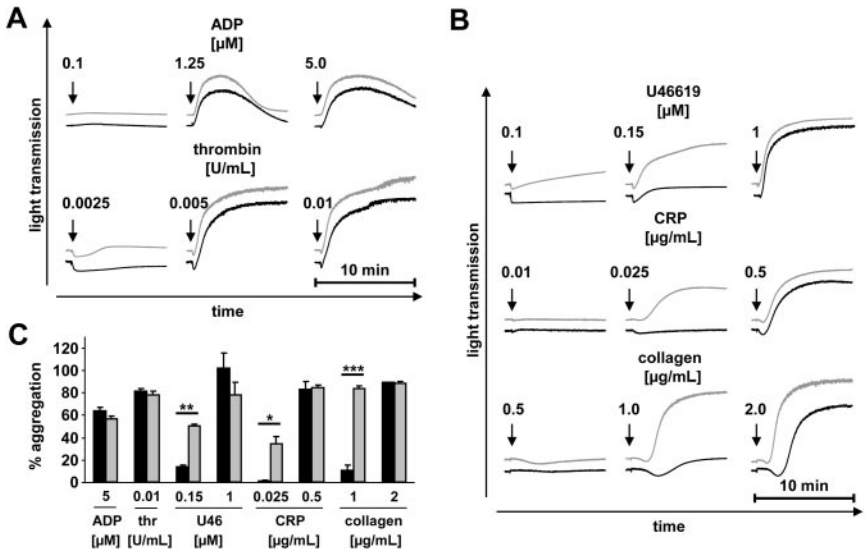

Figure 5. Enhanced aggregation of *Cdc42*$^{-/-}$ platelets at low agonist concentrations. (A-C) Aggregometry studies. prp from wild-type (■) or *Cdc42*$^{-/-}$ (▤) mice was stimulated with the indicated agonists; light transmission was recorded on a Fibrintimer 4 channel aggregometer. Thrombin measurements were performed using washed platelets. The results are representative of 3 individual experiments. (A-B) Representative aggregation curves. (C) Bar graphs of results obtained by aggregometry. Results are given as the mean percentage of aggregation ± SD. *P* values from left to right: **.002; *.032; ***< .001.

Cdc42$^{-/-}$ platelets form aggregates of increased size on collagen under flow

At sites of vessel wall injury, release of secondary mediators from activated platelets plays a crucial role for the recruitment and activation of further platelets to promote thrombus formation. To study the effect of enhanced degranulation of *Cdc42*$^{-/-}$ platelets on aggregate formation under flow, we perfused anticoagulated blood over a collagen-coated surface at a shear rate of 1000 seconds^{-1} (Figure 6). A moderate but significant increase in aggregate size of *Cdc42*$^{-/-}$ platelets compared with wild-type platelets was observed under these conditions (Figure 6A right panels), whereas the surface coverage was comparable between the 2 groups (Figure 6A left panels).

Cdc42$^{-/-}$ platelets display a decreased life span in vivo

Because *Cdc42*$^{-/-}$ platelets displayed mild thrombocytopenia, we determined the platelet life span in *Cdc42*$^{-/-}$ and wild-type mice in vivo (Figure 6B). For this, circulating platelets were labeled with a fluorescent noncytotoxic antibody derivative, and the labeled platelet population was monitored over time. After 1 hour (day 0), more than 90% of the circulating platelets in control and *Cdc42*$^{-/-}$ mice were labeled, and this platelet population gradually decreased over 5 days in wild-type mice, which is in agreement with the approximately 5-day life span of mouse platelets (Figure 6B). In contrast, a dramatically shortened life span was seen in *Cdc42*$^{-/-}$ mice, with a decrease to 39.8% plus or minus 7.6% and 0% on days 1 and 3, respectively. This result clearly demonstrates that although Cdc42 deficiency has only moderate effects on platelet function ex vivo, it significantly affects their homeostatic function in vivo, resulting in a markedly increased turnover, which may, at least in part, account for the moderate thrombocytopenia seen in these animals.

Accelerated arterial occlusive thrombus formation but prolonged bleeding times in *Cdc42*$^{-/-}$ mice

To investigate the effect of Cdc42 deficiency on thrombus formation in vivo, we monitored platelet accumulation at sites of ferric chloride–induced mesenteric arteriole injury using intravital fluorescence microscopy (Figure 7). Remarkably, although the beginning of thrombus formation followed similar kinetics in control and

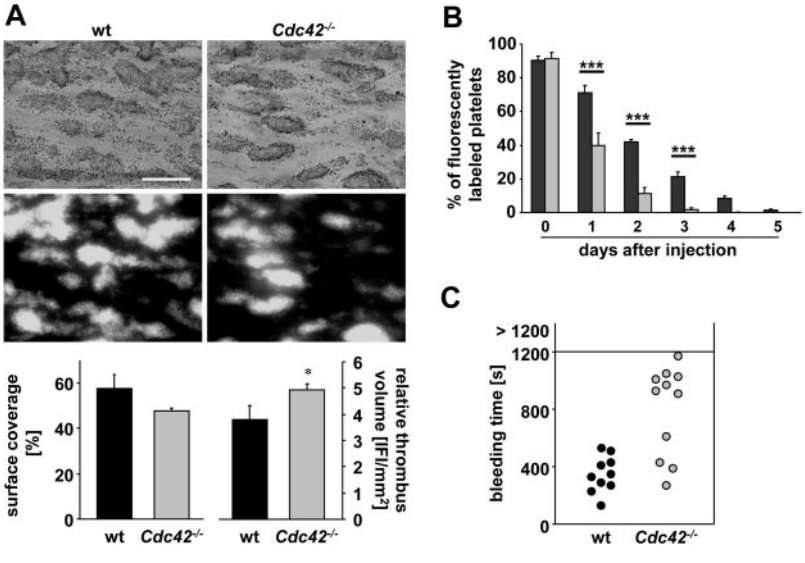

Figure 6. *Cdc42*$^{-/-}$ platelets form larger aggregates on collagen under flow. Whole blood from wild-type or *Cdc42*$^{-/-}$ mice was perfused over a collagen-coated surface (0.2 mg/mL) at a shear rate of 1000 seconds^{-1}. (A) Top row: representative phase contrast and fluorescence images of aggregate formation on collagen after 4 minutes of perfusion time. Scale bar equals 100 μm. Bottom row: mean surface coverage (left) and relative thrombus volume expressed as integrated fluorescence intensity (IFI) per square millimeter (right) ± SD of 6 mice per group. Left: wt, 57.58 ± 6.40; Cdc42$^{-/-}$, 47.72 ± 1.13 [%]; $P = .112$. Right: wt, 3.80 ± 0.54; Cdc42$^{-/-}$, 4.95 ± 0.20 [IFI/mm^2]; $^*P = .037$. (B) Decreased life span of *Cdc42*$^{-/-}$ platelets. Determination of the percentage of fluorescently labeled platelets of wild-type (■) and *Cdc42*$^{-/-}$ platelets (▤) for 5 days upon injection with 0.5 μg/g bodyweight GPIX-Dylight 488 derivate on day 0. ***$P < .001$. (C) Increased tail bleeding times in *Cdc42*$^{-/-}$ mice (●) compared with wild-type (●) mice. Each symbol represents 1 animal.

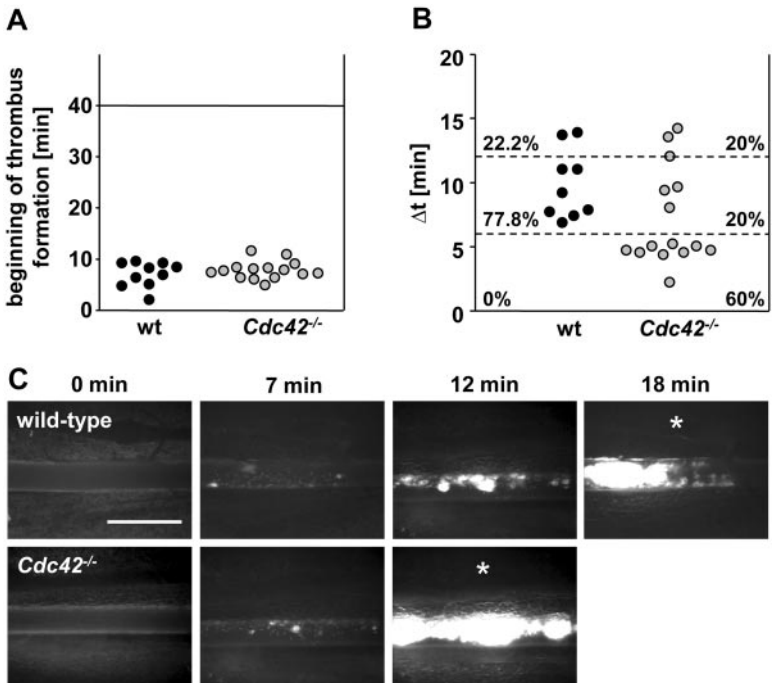

Figure 7. Accelerated thrombus formation in *Cdc42*$^{-/-}$ mice. (A-C) Mesenteric arterioles were injured with $FeCl_3$ and adhesion, and thrombus formation of fluorescently labeled platelets was monitored in vivo by fluorescence microscopy. (A) Time to appearance of first thrombus and (B) interval between start of thrombus formation and vessel occlusion are shown. Each symbol represents 1 animal. (C) Representative images are depicted. Scale bar equals 50 μm. White asterisks indicate occlusion of the vessel.

Cdc42-deficient mice (Figure 7A), the interval between the formation of first thrombi and complete occlusion of the respective arteriole was significantly shorter in Cdc42-deficient animals (Figure 7B) compared with wild-type controls. Within 6 minutes after appearance of the first thrombus larger than 10 μm, vessel occlusion occurred in 60% of the Cdc42-deficient animals (9 of 15), whereas no vessel occlusion was observed in arterioles of control mice during this time period.

To study the effect of Cdc42 deficiency on hemostasis, we performed tail bleeding experiments (Figure 6C). Very unexpectedly, a significant hemostatic defect was detectable in *Cdc42*$^{-/-}$ mice. Whereas bleeding stopped in all control mice within 10 minutes (mean, 5.9 ± 2.2 minutes), bleeding times were highly variable and generally increased in Cdc42-deficient animals (mean, 13.5 ± 5.3 minutes). However, all tested animals stopped bleeding within the observation period of 20 minutes.

Discussion

We have used a knockout approach to investigate the effect of Cdc42 deficiency on platelet function in vitro and in vivo. We found that megakaryocyte- and platelet-specific deletion of the *Cdc42* gene resulted in a complex phenotype, including mild thrombocytopenia, increased platelet size and, unexpectedly, increased secretion and a shortened platelet life span in mice. On the other hand, our results did not confirm the proposed major role of Cdc42 for filopodia formation in platelets.[33]

We show that Cdc42 is not required for platelet filopodia formation and full spreading on fibrinogen upon activation with thrombin (Figure 2A-B), as well as for morphologic changes under nonstimulating conditions (Figure 2C) or upon stimulation with ADP (data not shown), indicating the involvement of proteins other than Cdc42 in filopodia formation on fibrinogen under conditions of G protein–coupled signaling. This finding is in accordance with results from Czuchra et al, who—also using a genetic approach—have demonstrated that Cdc42 is dispensable for filopodia formation, migration, polarization, and mitosis in embryonic fibroblasts.[11] Recent data suggest the existence of Cdc42-independent mechanisms of filopodia formation, mainly involving the Rho GTPase Rif and LPR1.[5,10] Thus, one of these proteins may act in filopodia formation in *Cdc42*$^{-/-}$ platelets. Interestingly, our studies of platelet ultrastructure revealed no differences in filopodia morphology between *Cdc42*$^{-/-}$ and wild-type platelets upon activation (Figure 3B-C), whereas filopodia induced by Rif and LPR1 were shown to have a longer and more hairy appearance than those induced by Cdc42.[5,9] Thus, further studies are required to identify the mechanisms underlying filopodia formation in platelets.

Notably, however, *Cdc42*$^{-/-}$ platelets displayed a clear defect in GPIb signaling-dependent filopodia formation induced by adhesion on VWF (Figure 3D), which was most likely not caused by decreased GPIb expression levels because agglutination induced by botrocetin and human VWF was unaltered in the mutant cells (Figure 3E). This finding is intriguing because it establishes Cdc42 as a GPIb-specific downstream-signaling molecule. A role of Cdc42 in platelet filopodia formation has been previously proposed downstream of the human platelet integrin $\alpha_6\beta_1$ using secramine A as a Cdc42-specific inhibitor.[33] We found that secramine A also prevented the GPIb-dependent response (data not shown), but nonspecific effects of this compound were suggested by its ability to induce shape change in resting platelets. The signaling pathway downstream of GPIb leading to filopodia formation remains to be fully characterized. Under our assay condition, which prevents signal amplification by $\alpha_{IIb}\beta_3$ integrin, ADP, or TXA_2, the signaling response evoked by GPIb involves calcium mobilization from intracellular stores downstream of a src kinase and PLCγ2.[36] These effectors are not restricted to GPIb signaling but also take part in GPVI and Fc receptor/ITAM-dependent activation. An increased rather than decreased response of *Cdc42*$^{-/-}$ platelets to CRP and collagen and unaltered filopodia formation upon static adhesion to CRP observed here further supports the notion of a GPIb-restricted role of Cdc42 and indicates the existence of a separate pathway unrelated to those induced by ITAM-coupled receptors. Our finding is consistent with reports showing biochemical and functional interaction of Cdc42 with 2 known GPIb partners, filamin[37] and 14-3-3.[38]

Unexpectedly, *Cdc42*$^{-/-}$ platelets did not display decreased, but rather increased secretion in response to agonist stimulation (Figure 4). A significant increase in P-selectin expression and PF4 release despite unaltered protein content strongly indicates enhanced secretion of α granules in *Cdc42*$^{-/-}$ platelets (Figure 4A bottom panel; Figure 4B). In contrast, the observed strong increase of dense granule–dependent ATP release coincided with a significantly increased ADP/ATP content in the mutant platelets that may only partially be explained by their increased size because content and release of the dense granular mediator serotonin was not significantly altered (Figures 1C-D, 4C; Table 1; supplemental Figure 2D-E). Thus, the increase in ADP/ATP content might contribute to the hyperreactivity observed in aggregometry, where released mediators accumulate and to a great extent reinforce platelet activation and secretion. However, Cdc42 may also have a direct function in the degranulation machinery, as increased P-selectin exposure was observed also in flow cytometric studies (Figure 4A bottom panel), where highly diluted platelet samples are analyzed under conditions that minimize the influence of released mediators on the activation state of the cells.[39]

Our results stand in contrast to studies by Pula et al, who found that platelets treated with secramine A show a selective aggregation and adhesion defect in response to collagen.[40] This discrepancy is difficult to explain at present, but it might be related to limited specificity of the inhibitor. The increased secretion in *Cdc42*$^{-/-}$ platelets stands in clear contrast to observations made in other cell types showing decreased exocytosis upon inhibition of Cdc42, including endothelial cells and mast cells.[17,19,20] This indicates that Cdc42 might fulfill multiple functions that may differ between cell types or, alternatively, methodologic differences may account for the discrepant results. We have used a direct genetic approach to delete Cdc42 expression/function in vivo, whereas all studies mentioned here used cell-culture systems and transfection models. Notably, Czuchra et al showed that expression of dominant-negative Cdc42 in Cdc42-null cells most likely resulted in the inhibition of other Rho GTPases, thereby significantly influencing the observed phenotype.[11] This finding is in accordance with the observation by Hong-Geller et al, who indeed found an unexplained decrease in exocytosis when overexpressing wild-type Cdc42 in RBL mast cells.[19]

Cdc42$^{-/-}$ platelets formed larger aggregates on collagen under flow in vitro (Figure 6A). Similarly, we found thrombus formation in *Cdc42*$^{-/-}$ mice to be significantly accelerated in an arterial injury model in vivo compared with wild-type platelets (Figure 7). Considering the increased secretion observed in *Cdc42*$^{-/-}$ platelets in vitro, one might speculate that this effect was caused by the increased presence of platelet-released thrombogenic factors at the site of injury. This notion would be in line with studies from other groups demonstrating the significance of degranulation-dependent release of platelet agonists, such as ADP and ATP, for thrombus formation under physiologic conditions.[3,41,42] Furthermore, our results clearly show that effective thrombus formation can still take place under conditions of decreased circulating platelet numbers.[43] In contrast to these observations, Cdc42-deficient mice displayed variable but significantly prolonged bleeding times, indicating impaired platelet plug formation (Figure 6C). Possibly, the impaired GPIb-dependent signaling (Figure 3D) contributes to this effect. Furthermore, decreased GPIb expression levels and decreased integrin $\alpha_{IIb}\beta_3$ activation in *Cdc42*$^{-/-}$ platelets may also influence their function in this assay.[44] It is difficult to explain these opposite effects of Cdc42 deficiency on platelet function in vivo, but a different relative importance of individual molecular pathways for plug formation in the tail bleeding assay on the one hand and models of occlusive arterial thrombus formation on the other hand has been shown before.[45-47]

Our results indicate a novel regulatory role for Cdc42 in platelet activatory/secretory events in vitro and in vivo. Importantly, increased secretion of *Cdc42*$^{-/-}$ platelets was not restricted to a specific agonist but occurred in response to G protein–coupled agonists as well as ITAM-coupled agonists, indicating a general function of the Cdc42 protein in platelet granule content organization and degranulation. In line with this, the increased ADP/ATP content suggests that Cdc42 may be required for proper granule formation/packing during platelet production. Moreover the increased P-selectin expression and PF4 release in *Cdc42*$^{-/-}$ platelets indicate that Cdc42 deficiency directly leads to enhanced secretion of α granules in platelets. At present, the exact role of the regulation of actin cytoskeleton in exocytotic events in platelets is controversial. Several studies using actin-disrupting agents supported a model in which the cytoskeleton in resting platelets may act as a barrier for granule release, and that platelet activation leads to (partial) disrupture of actin filaments, thereby enabling degranulation.[48] However, this model is questioned because of the risk of artefacts caused by actin-disrupting agents. To test a possible effect of Cdc42 deficiency on agonist-induced cytoskeletal rearrangements, we examined the Cdc42 downstream effector cofilin, a protein known to be involved in increasing actin turnover in its active dephosphorylated form.[49] Unexpectedly, and in contrast to the currently proposed function of Cdc42,[50] we found not a decrease, but a strong (~ 2-fold) increase in the (inactive) phosphorylated cofilin form in resting *Cdc42*$^{-/-}$ platelets compared with controls (supplemental Figure 3). This finding is in accordance with a recent study showing increased cofilin phosphorylation in cortical neurons upon genetic Cdc42 deletion.[51] Thrombin- and CRP-induced dephosphorylation of cofilin occurred to a similar extent and with similar kinetics in wild-type and *Cdc42*$^{-/-}$ platelets, although higher levels of the inactive, phosphorylated form of the protein were consistently detected in the mutant cells under all experimental conditions (data not shown). Furthermore, we found similar levels of F-actin in resting and thrombin-activated *Cdc42*$^{-/-}$ and wild-type platelets (data not shown), indicating that a reorganization rather than a disassembly of actin might be responsible for the cytoskeletal effects evoked by Cdc42 deficiency, but further studies will be required to test this hypothesis.

In addition to actin remodeling, Cdc42 could also participate directly or indirectly in the exocytotic processes in platelets. Recently, it became evident that platelets possess a secretory machinery similar to that of other cell types.[52] Thus, Cdc42 may evoke differential signaling events during platelet exocytosis that may be of importance for rapid but controlled platelet degranulation upon activation.

Our study has revealed multiple and novel roles for Cdc42 during platelet activation and granule organization/exocytosis, whereas we could not confirm its proposed essential role for filopodia formation in the cells except under conditions of selective GPIb dependent activation. These findings point to Cdc42 and/or its downstream effector molecules as potential targets for the development of novel drugs for the regulation of intravascular platelet activation.

Acknowledgments

We thank Dr Radek Skoda for kindly providing the PF4-Cre mice, Drs Cécile Denis and Peter Lenting for providing murine recombinant VWF, and Steffi Hartmann and Juliana Goldmann for excellent technical assistance.

This work was supported by the DFG (Sonderforschungsbereich 688) and the Rudolf Virchow Center.

Authorship

Contribution: I.P. performed experiments, analyzed data, and contributed to the writing of the paper; A.E., M.E., I.H., S.E., and M.B. performed experiments and analyzed data; X.W. and C.B. provided vital new reagents and contributed to the writing of the paper; F.L. and C.G. analyzed data and contributed to the writing of the paper; and B.N. designed research, analyzed data, and wrote the paper.

Conflict-of-interest disclosure: The authors declare no competing financial interests.

Correspondence: Bernhard Nieswandt, Chair of Vascular Medicine, Rudolf Virchow Center, DFG Research Center for Experimental Biomedicine, University Clinic Würzburg, Josef-Schneider-Str 2, 97080 Würzburg, Germany; e-mail: bernhard.nieswandt@virchow.uni-wuerzburg.de.

References

1. Nobes CD, Hall A. Rho, rac, and cdc42 GTPases regulate the assembly of multimolecular focal complexes associated with actin stress fibers, lamellipodia, and filopodia. *Cell.* 1995;81(1):53-62.
2. Offermanns S. Activation of platelet function through G protein-coupled receptors. *Circ Res.* 2006;99(12):1293-1304.
3. Pleines I, Elvers M, Strehl A, et al. Rac1 is essential for phospholipase C-gamma2 activation in platelets. *Pflugers Arch.* 2009;457(5):1173-1185.
4. Jaffe AB, Hall A. Rho GTPases: biochemistry and biology. *Annu Rev Cell Dev Biol.* 2005;21:247-269.
5. Sigal YJ, Quintero OA, Cheney RE, Morris AJ. Cdc42 and ARP2/3-independent regulation of filopodia by an integral membrane lipid-phosphatase-related protein. *J Cell Sci.* 2007;120(2):340-352.
6. Bear JE, Svitkina TM, Krause M, et al. Antagonism between Ena/VASP proteins and actin filament capping regulates fibroblast motility. *Cell.* 2002;109(4):509-521.
7. Welch MD, Mullins RD. Cellular control of actin nucleation. *Annu Rev Cell Dev Biol.* 2002;18:247-288.
8. Krugmann S, Jordens I, Gevaert K, et al. Cdc42 induces filopodia by promoting the formation of an IRSp53:Mena complex. *Curr Biol.* 2001; 11(21):1645-1655.
9. Pellegrin S, Mellor H. The Rho family GTPase Rif induces filopodia through mDia2. *Curr Biol.* 2005; 15(2):129-133.
10. Ellis S, Mellor H. The novel Rho-family GTPase rif regulates coordinated actin-based membrane rearrangements. *Curr Biol.* 2000;10(21):1387-1390.
11. Czuchra A, Wu X, Meyer H, et al. Cdc42 is not essential for filopodium formation, directed migration, cell polarization, and mitosis in fibroblastoid cells. *Mol Biol Cell.* 2005;16(10):4473-4484.
12. Malacombe M, Ceridono M, Calco V, et al. Intersectin-1L nucleotide exchange factor regulates secretory granule exocytosis by activating Cdc42. *EMBO J.* 2006;25(15):3494-3503.
13. Momboisse F, Ory S, Calco V, et al. Calcium-regulated exocytosis in neuroendocrine cells: intersectin-1L stimulates actin polymerization and exocytosis by activating Cdc42. *Ann NY Acad Sci.* 2009;1152:209-214.
14. Nevins AK, Thurmond DC. Glucose regulates the cortical actin network through modulation of Cdc42 cycling to stimulate insulin secretion. *Am J Physiol Cell Physiol.* 2003;285(3):C698-C710.
15. Nevins AK, Thurmond DC. A direct interaction between Cdc42 and vesicle-associated membrane protein 2 regulates SNARE-dependent insulin exocytosis. *J Biol Chem.* 2005;280(3):1944-1952.
16. Wang Z, Oh E, Thurmond DC. Glucose-stimulated Cdc42 signaling is essential for the second phase of insulin secretion. *J Biol Chem.* 2007;282(13):9536-9546.
17. Klarenbach SW, Chipiuk A, Nelson RC, Hollenberg MD, Murray AG. Differential actions of PAR2 and PAR1 in stimulating human endothelial cell exocytosis and permeability: the role of Rho-GTPases. *Circ Res.* 2003;92(3):272-278.
18. Hobert ME, Sands KA, Mrsny RJ, Madara JL. Cdc42 and Rac1 regulate late events in Salmonella typhimurium-induced interleukin-8 secretion from polarized epithelial cells. *J Biol Chem.* 2002; 277(52):51025-51032.
19. Hong-Geller E, Cerione RA. Cdc42 and Rac stimulate exocytosis of secretory granules by activating the IP(3)/calcium pathway in RBL-2H3 mast cells. *J Cell Biol.* 2000;148(3):481-494.
20. Hong-Geller E, Holowka D, Siraganian RP, Baird B, Cerione RA. Activated Cdc42/Rac reconstitutes Fcepsilon RI-mediated Ca2+ mobilization and degranulation in mutant RBL mast cells. *Proc Natl Acad Sci U S A.* 2001;98(3):1154-1159.
21. Ren Q, Ye S, Whiteheart SW. The platelet release reaction: just when you thought platelet secretion was simple. *Curr Opin Hematol.* 2008;15(5):537-541.
22. White JG, Burris SM. Morphometry of platelet internal contraction. *Am J Pathol.* 1984;115(3): 412-417.
23. White JG, Krivit W. Fine structural localization of adenosine triphosphatase in human platelets and other blood cells. *Blood.* 1965;26(3):554-568.
24. Wu X, Quondamatteo F, Lefever T, et al. Cdc42 controls progenitor cell differentiation and beta-catenin turnover in skin. *Genes Dev.* 2006;20(5): 571-585.
25. Tiedt R, Schomber T, Hao-Shen H, Skoda RC. Pf4-Cre transgenic mice allow the generation of lineage-restricted gene knockouts for studying megakaryocyte and platelet function in vivo. *Blood.* 2007;109(4):1503-1506.
26. Andrews RK, Booth WJ, Gorman JJ, Castaldi PA, Berndt MC. Purification of botrocetin from *Bothrops jararaca* venom: analysis of the botrocetin-mediated interaction between von Willebrand factor and the human platelet membrane glycoprotein Ib-IX complex. *Biochemistry.* 1989; 28(12):8317-8326.
27. Knight CG, Morton LF, Onley DJ, et al. Collagen-platelet interaction: Gly-Pro-Hyp is uniquely specific for platelet Gp VI and mediates platelet activation by collagen. *Cardiovasc Res.* 1999;41(2): 450-457.
28. Nieswandt B, Bergmeier W, Rackebrandt K, Gessner JE, Zirngibl H. Identification of critical antigen-specific mechanisms in the development of immune thrombocytopenic purpura in mice. *Blood.* 2000;96(7):2520-2527.
29. Nieswandt B, Brakebusch C, Bergmeier W, et al. Glycoprotein VI but not alpha2beta1 integrin is essential for platelet interaction with collagen. *EMBO J.* 2001;20(9):2120-2130.
30. Léon C, Hechler B, Vial C, et al. The P2Y1 receptor is an ADP receptor antagonized by ATP and expressed in platelets and megakaryoblastic cells. *FEBS Lett.* 1997;403(1):26-30.
31. May F, Hagedorn I, Pleines I, et al. CLEC-2 is an essential platelet activating receptor in hemostasis and thrombosis. *Blood.* 2009;114(16):3464-3472.
32. Chen F, Ma L, Parrini MC, et al. Cdc42 is required for PIP(2)-induced actin polymerization and early development but not for cell viability. *Curr Biol.* 2000;10(13):758-765.
33. Chang JC, Chang HH, Lin CT, Lo SJ. The integrin alpha6beta1 modulation of PI3K and Cdc42 activities induces dynamic filopodium formation in human platelets. *J Biomed Sci.* 2005;12(6):881-898.
34. Yuan Y, Kulkarni S, Ulsemer P, et al. The von Willebrand factor-glycoprotein Ib/V/IX interaction induces actin polymerization and cytoskeletal reorganization in rolling platelets and glycoprotein Ib/V/IX-transfected cells. *J Biol Chem.* 1999; 274(51):36241-36251.
35. Bergmeier W, Schulte V, Brockhoff G, et al. Flow cytometric detection of activated mouse integrin alphaIIbbeta3 with a novel monoclonal antibody. *Cytometry.* 2002;48(2):80-86.
36. Mangin P, Yuan Y, Goncalves I, et al. Signaling role for phospholipase C gamma 2 in platelet glycoprotein Ib alpha calcium flux and cytoskeletal reorganization: involvement of a pathway distinct from FcR gamma chain and Fc gamma RIIA. *J Biol Chem.* 2003;278(35): 32880-32891.
37. Ohta Y, Suzuki N, Nakamura S, Hartwig JH, Stossel TP. The small GTPase RalA targets filamin to induce filopodia. *Proc Natl Acad Sci U S A.* 1999;96(5):2122-2128.
38. Bialkowska K, Zaffran Y, Meyer SC, Fox JE. 14-3-3 zeta mediates integrin-induced activation of Cdc42 and Rac: platelet glycoprotein Ib-IX regulates integrin-induced signaling by sequestering 14-3–3 zeta. *J Biol Chem.* 2003;278(35):33342-33350.
39. Nieswandt B, Schulte V, Zywietz A, Gratacap MP, Offermanns S. Costimulation of Gi- and G12/G13-mediated signaling pathways induces integrin alpha IIbbeta 3 activation in platelets. *J Biol Chem.* 2002;277(42):39493-39498.
40. Pula G, Poole AW. Critical roles for the actin cytoskeleton and cdc42 in regulating platelet integrin alpha2beta1. *Platelets.* 2008;19(13):199-210.
41. Remijn JA, Wu YP, Jeninga EH, et al. Role of ADP receptor P2Y(12) in platelet adhesion and thrombus formation in flowing blood. *Arterioscler Thromb Vasc Biol.* 2002;22(4):686-691.
42. Konopatskaya O, Gilio K, Harper MT, et al. PKCalpha regulates platelet granule secretion and thrombus formation in mice. *J Clin Invest.* 2009; 119(2):399-407.
43. Grosse J, Braun A, Varga-Szabo D, et al. An EF hand mutation in Stim1 causes premature platelet activation and bleeding in mice. *J Clin Invest.* 2007;117(11):3540-3550.
44. Scarborough RM, Kleiman NS, Phillips DR. Platelet glycoprotein IIb/IIIa antagonists: what are the

relevant issues concerning their pharmacology and clinical use? *Circulation*. 1999;100(4):437-444.

45. Ni H, Yuen PS, Papalia JM, et al. Plasma fibronectin promotes thrombus growth and stability in injured arterioles. *Proc Natl Acad Sci U S A*. 2003;100(5):2415-2419.
46. Renné T, Pozgajova M, Gruner S, et al. Defective thrombus formation in mice lacking coagulation factor XII. *J Exp Med*. 2005;202(2):271-281.
47. Elvers M, Stegner D, Hagedorn I, et al. Impaired alpha(IIb)beta(3) integrin activation and shear-dependent thrombus formation in mice lacking phospholipase D1. *Sci Signal*. 2010; 3(103):ra1.
48. Flaumenhaft R, Dilks JR, Rozenvayn N, et al. The actin cytoskeleton differentially regulates platelet alpha-granule and dense-granule secretion. *Blood*. 2005;105(10):3879-3887.
49. Bamburg JR. Proteins of the ADF/cofilin family: essential regulators of actin dynamics. *Annu Rev Cell Dev Biol*. 1999;15:185-230.
50. Wang W, Eddy R, Condeelis J. The cofilin pathway in breast cancer invasion and metastasis. *Nat Rev Cancer*. 2007;7(6):429-440.
51. Garvalov BK, Flynn KC, Neukirchen D, et al. Cdc42 regulates cofilin during the establishment of neuronal polarity. *J Neurosci*. 2007;27(48): 13117-13129.
52. Polgár J, Chung SH, Reed GL. Vesicle-associated membrane protein 3 (VAMP-3) and VAMP-8 are present in human platelets and are required for granule secretion. *Blood*. 2002; 100(3):1081-1083.